The main sequence view of quasars accreting at high rates: influence of star formation[*]

PAOLA MARZIANI [ID],[1] MARZENA SNIEGOWSKA [ID],[2] SWAYAMTRUPTA PANDA [ID],[2]
BOŻENA CZERNY [ID],[2] C. ALENKA NEGRETE [ID],[3] DEBORAH DULTZIN [ID],[3]
KARLA GARNICA,[3] MARY LOLI MARTÍNEZ-ALDAMA [ID],[2] ASCENSIÓN DEL OLMO [ID],[4]
MAURO D'ONOFRIO [ID],[5] ALICE DECONTO MACHADO [ID][4] AND VALERIO GANCI[6]

(THE EXTREME TEAM)

[1] *National Institute for Astrophysics (INAF), Astronomical Observatory of Padova, Padova, Italy*
[2] *Center for Theoretical Physics (PAS), Warsaw, Poland*
[3] *Universidad Nacional Autonóma de México Instituto de Astronomía, Mexico*
[4] *Instituto de Astrofisíca de Andalucía, IAA-CSIC, Granada, Spain*
[5] *Dipartimento di Fisica e Astronomia, Università di Padova, Padova, Italy*
[6] *Institute of Physics, University of Cologne, Germany*

ABSTRACT

Highly-accreting quasars show fairly distinctive properties in their optical, UV, and X spectra, and are easy to recognize because of their specific location in the quasar main sequence: they are the strongest optical FeII emitters. They show a surprisingly high rate of radio detections and, at variance with the classical radio-loud (jetted) sources, the origin of their radio emission is probably thermal. The chemical composition of the broad line emitting gas implies high metallicity values, above 10 times solar. A fraction of highly-accreting quasars at intermediate and high redshift might therefore be in a particular evolutionary stage that is unobscured albeit still involving a contribution of nuclear and circum-nuclear star formation in their multifrequency properties.

1. INTRODUCTION

Corresponding author: Paola Marziani
paola.marziani@inaf.it

[*] Contribution presented at the 237th meeting of the AAS.

The quasar main sequence (MS; e.g., Sulentic et al. 2000; Shen & Ho 2014; Marziani et al. 2018) organizes sources on the basis of the line width and prominence of singly ionized iron emission. A sketch of the MS of quasars is shown in Figure 1, adapted from Ganci et al. (2019). The shape of the main sequence makes it possible to subdivide quasar samples in a succession of spectral types. Quasars with strong optical singly-ionized iron emission i.e., with $R_{\mathrm{FeII}} \gtrsim 1$ (where the parameter R_{FeII} is defined by the intensity ratio between the FeII emission blend at $\lambda 4570$ Å and Hβ, Boroson & Green 1992) are believed to be sources accreting at very high rate (possibly super-Eddington) and radiating close to a maximum permitted Eddington ratio (Shen & Liu 2012; Du et al. 2016). They show a high fraction (≈ 30 %) of radio-detected sources, even if they are at the opposite end of the MS location expected for classical radio-loud objects (jetted; Padovani 2017, see Fig. 1 and Zamfir et al. 2008). In the most extreme cases, their radio power can reach values comparable to the ones of relativistically jetted sources ($\sim 5 \cdot 10^{24}$ W Hz^{-1}).

2. RESULTS

2.1. *Radio emission from the host galaxy*

Quasars with highly accreting black holes identified from their MS location follow the correlation between FIR luminosity and radio-power of star forming galaxies and radio quiet quasars. Fig. 1 shows that the star formation rate (SFR) computed from radio power and FIR luminosity are correlated, and that their values are consistent with the location expected for radio-quiet quasars. Radio properties are consistent with emission from sources whose origin is thermal," i.e. most likely the integrated emission of supernova remnants, following a period of intense star formation.

2.2. *High metal content in the Broad Line Region*

We carried out an explorative analysis of the UV spectra of intermediate redshift quasars. We estimated metallicity from diagnostic ratios between the UV resonance lines of Carbon, Aluminium and Silicon at $\lambda 1549$, $\lambda 1860$ and $\lambda 1397$ and the HeII line at $\lambda 1640$ Å. The diagnostic line intensity ratios computed separately for a wind (blueshifted with respect to the quasar rest frame) and a virialized (unshifted) emission line component allow for the determination of a restricted volume in the 3D parameter space metallicity, ionization parameter, and density by comparing the observed values with the predictions of photoionization simulations computed with CLOUDY 17.02 (Ferland et al. 2017). The derived metallicity values are high (typically around 2050 times solar) and probably the highest along the quasar main sequence, if abundance ratios of Aluminium and Silicon scale as solar with respect to Carbon (Śniegowska et al. 2020). Fig. 1 shows the case of quasar SDSS J1024421.32+024520.2 whose metal line ratios with HeII $\lambda 1640$ are close to the median values of the sample of Śniegowska et al. (2020). The contour line delimits the region consistent with the minimum χ^2 within 1σ confidence level.
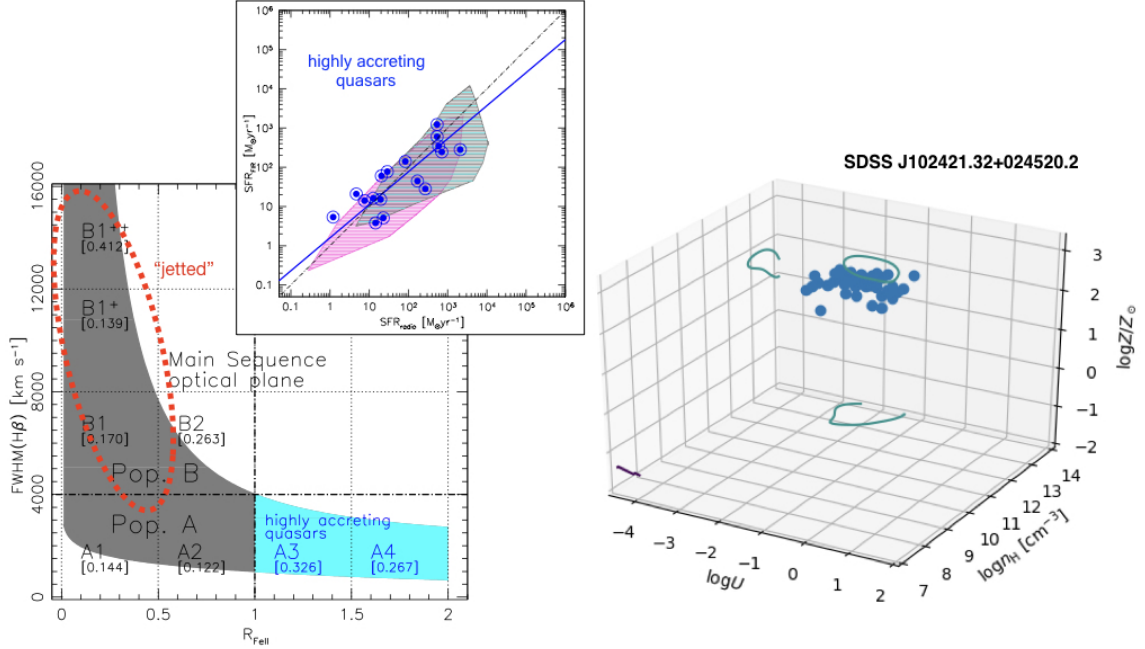
Figure 1. Left panel: sketch of the MS of quasar and identification of the spectral types, as a function of FWHM(Hβ) vs. R_{FeII}. Gray and cyan areas trace the source occupation in the plane. Numbers yield the fraction of sources in each spectral bin that are radio detected (including radio-intermediate and radio-loud) in the Faint Images of the Radio Sky at Twenty-Centimeters (FIRST, Becker et al. 1995 survey for an optically selected sample of 680 sources at redshift $z \lesssim 1$ (Marziani et al. 2013). The dashed line approximately delimits the region where relativistic jetted quasars are found (Zamfir et al. 2008). Inset panel: the correlation between SFR derived from radio power and FIR luminosity for a set of highly-accreting sources (blue circles) over a broad range of redshift, adapted from Ganci et al. (2019) and del Olmo et al. (2021). The shaded areas identify the loci for star-forming galaxies (glycine) and for radio-quiet quasars (cyan). Right panel: parameter space ionization parameter U, Hydrogen density and metallicity Z. The region of the parameter space where observed diagnostic intensity ratios measured on the spectrum of the quasar SDSS J102421.32+024520.2 are in agreement with photoionization predictions is delimited by contour lines.

3. DISCUSSION AND CONCLUSION

The early stages in the evolution of AGN and quasars may involve merging and strong gravitational interaction, leading to accumulation of gas in the galaxy central regions, and inducing a burst of star formation. Mass loss due to stellar winds and supernova explosions eventually provides accretion fuel for the massive black hole at the galaxy center. Radiation and pressure forces can then sweep the dust and gas surrounding the black hole, at least within a cone coaxial with the accretion disk axis from where the radiative and mechanical output is free to escape into the host

galaxy ISM (a sketch of this scenario is provided by D'Onofrio & Marziani 2018). Since the quasars in our samples are essentially unobscured or almost so, radiation and mechanical forces from their outflows must have already swept away the cocoon of gas and dust surrounding the accreting black hole in the early stages of the quasar evolution, at least within a cone coaxial within the accretion disk axis. The extreme accretors in our sample have emerged from the obscured phase, but are still affected by recent star formation in the chemical composition of the line emitting gas and by host galaxy star formation. The most luminous ones meet the definition of cold quasars (Kirkpatrick et al. 2020), with SFR in excess of 200 $M_\odot$ yr^{-1}.

ACKNOWLEDGMENTS

REFERENCES

Becker, R. H., White, R. L., & Helfand, D. J. 1995, ApJ, 450, 559, doi: 10.1086/176166

Boroson, T. A., & Green, R. F. 1992, ApJS, 80, 109, doi: 10.1086/191661

del Olmo, A., Marziani, P., Ganci, V., et al. 2021, Proceedings of the International Astronomical Union, 356, 310

D'Onofrio, M., & Marziani, P. 2018, Frontiers in Astronomy and Space Sciences, 5, 31, doi: 10.3389/fspas.2018.00031

Du, P., Lu, K.-X., Hu, C., et al. 2016, ApJ, 820, 27, doi: 10.3847/0004-637X/820/1/27

Ferland, G. J., Chatzikos, M., Guzmán, F., et al. 2017, RMxAA, 53, 385. https://arxiv.org/abs/1705.10877

Ganci, V., Marziani, P., D'Onofrio, M., et al. 2019, A&A, 630, A110, doi: 10.1051/0004-6361/201936270

Kirkpatrick, A., Urry, C. M., Brewster, J., et al. 2020, ApJ, 900, 5, doi: 10.3847/1538-4357/aba358

Marziani, P., Sulentic, J. W., Plauchu-Frayn, I., & del Olmo, A. 2013, AAp, 555, 89, 16pp. https://arxiv.org/abs/1305.1096

Marziani, P., Dultzin, D., Sulentic, J. W., et al. 2018, Frontiers in Astronomy and Space Sciences, 5, 6. https://arxiv.org/abs/1802.05575

Padovani, P. 2017, Frontiers in Astronomy and Space Sciences, 4, 35, doi: 10.3389/fspas.2017.00035

Shen, Y., & Ho, L. C. 2014, Nature, 513, 210, doi: 10.1038/nature13712

Shen, Y., & Liu, X. 2012, ApJ, 753, 125, doi: 10.1088/0004-637X/753/2/125

Śniegowska, M., Marziani, P., Czerny, B., et al. 2020, arXiv e-prints, arXiv:2009.14177. https://arxiv.org/abs/2009.14177

Sulentic, J. W., Marziani, P., & Dultzin-Hacyan, D. 2000, ARA&A, 38, 521, doi: 10.1146/annurev.astro.38.1.521

Zamfir, S., Sulentic, J. W., & Marziani, P. 2008, MNRAS, 387, 856, doi: 10.1111/j.1365-2966.2008.13290.x